Environmental Modeling

Microbial turnover of glyphosate to biomass: utilization as nutrient source, formation of AMPA and biogenic NER in an OECD 308 test

Andreas Libonati Brock, Arno Rein, Fabio Polesel, Karolina Malgorzata Nowak, Matthias Kästner, and Stefan Trapp

Environ. Sci. Technol., **Just Accepted Manuscript** • DOI: 10.1021/acs.est.9b01259 • Publication Date (Web): 17 Apr 2019

Microbial turnover of glyphosate to biomass: utilization as nutrient source, formation of AMPA and biogenic NER in an OECD 308 test

Andreas Libonati Brock[1], Arno Rein[2], Fabio Polesel[1], Karolina M. Nowak[3], Matthias Kästner[3*], Stefan Trapp[1]

[1]Department of Environmental Engineering, Technical University of Denmark, Bygningstorvet 115, 2800 Kgs. Lyngby, Denmark

[2]Chair of Hydrogeology, Technical University of Munich, Arcisstrasse 21, Munich 80333, Germany

[3]Helmholtz-Centre for Environmental Research − UFZ, Department of Environmental Biotechnology, Permoserstrasse 15, 04318 Leipzig, Germany

Corresponding author:

Matthias Kästner, e-mail: matthias.kaestner@ufz.de, phone: +49 341/235-1235; Fax: +49 341/235-451235

18 **TOC Art**

19

20 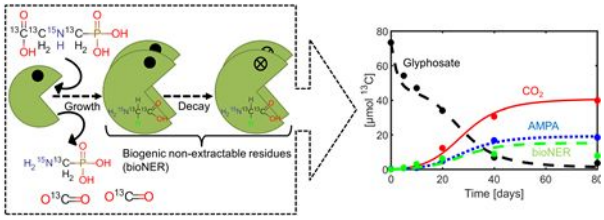

Abstract

Environmental fate assessment of chemicals involves standardized simulation tests with isotope-labeled molecules to balance transformation, mineralization, and formation of non-extractable residues (NER). Methods to predict microbial turnover and biogenic NER have been developed, having limited use when metabolites accumulate, the chemicals are not the only C source, or provides for other macro-elements. To improve predictive capability, we extended a recently developed method for microbial growth yield estimation for incomplete degradation and multiple-element assimilation and combined it with a dynamic model for fate description in soils and sediments. We evaluated the results against the unique experimental data of $^{13}C_3$-^{15}N-co-labelled glyphosate turnover with AMPA formation in water-sediment systems (OECD 308). Balancing ^{13}C- and ^{15}N- fluxes to biomass, showed a pronounced shift of glyphosate transformation from full mineralization to AMPA formation. This may be explained by various hypotheses, e.g. the limited substrate turnover inherent to the batch conditions of the test system causing microbial starvation or inhibition by P release. Modeling results indicate initial N overload due to the lower C/N ratio in glyphosate compared to average cell composition leading to subsequent C demand and accumulation of AMPA.

Keywords: bound residues, Gibbs Free Energy, microbial growth yield, non-extractable residues, simulation, aminomethylphosphonic acid

1 Introduction

All chemicals sold commercially in the European Union (EU) require approval under the EU chemicals legislation REACH[1]. Standardized simulation tests (e.g. OECD tests 307[2] and 308[3]) applying radio- or stable isotope labeled molecules in water, soils, and sediments are used for gaining sufficient information about the general environmental fate and persistence.[4,5] However, there is still a debate about interpreting OECD 308 tests combining gas-water-sediment interfaces, in particular if the deviation of DegT50 (which is the time until 50% of the parent chemical is degraded) in water and sediments is considered.[3,6–8] In these tests, the turnover is balanced between mineralization, transformation products and the formation of non-extractable residues (NER).

Particular focus for persistence assessment of a chemical is on the formation of NER, which are always formed during such simulation tests,[9] and can be the largest fraction (up to 90%) of initial label mass at the end of a test.[10] NER are determined by the presence of the isotope label after exhaustive extractions of solid matrices (sediment, soil, sludge, suspended particles etc.) with limited information about their speciation.[9,11,12] Until recently, neither the potential risk nor the composition of the NER could be reliably determined.[9] The limited knowledge of the NER speciation resulted in conflicting conclusions regarding the persistence of the active parent chemicals.[5,13,14] Previous NER definitions have promoted a mismatch between the legislation and the state of knowledge in research and modeling. Only parent compounds and primary metabolites are defined as NER, whereas label conversion to natural bio-components (bioNER), which pose no risk, is explicitly excluded e.g. in the widely accepted definition of Roberts.[15] However, NER assessment based on the remaining isotope labels always include bioNER thus resulting in an overestimation of the potential risks and persistence.[3,6]

Recent advances in analytical methods and theories have helped elucidating the nature and composition of NER and identified bioNER as a major fraction of the formed NER.[9,11,12,16–19] This has improved the knowledge obtained from OECD tests regarding the potential risks to the environment and human health.[5] Recently, a method for predicting microbial growth yields of chemicals (Microbial Turnover to Biomass, MTB) was developed[20] providing the opportunity to estimate the potential bioNER formation. This method has been applied to estimate bioNER formed from 40 chemicals of environmental concern[21] and, in addition, to predict input parameters for use in the 'unified model for biodegradation and sorption'.[20] With the MTB method, the microbial growth yield can be predicted under the assumption of complete mineralization of the parent compound with productive growth for various terminal electron acceptors (O_2, NO_3^-, SO_4^{2-}). However, metabolites may accumulate diminishing both the matter flux of macro-elements (C, N, P) and the energy gain of the microorganism, eventually resulting in lower growth yields. To date,

the MTB method considered the substrate use as C and energy source for the microorganisms while certain substrates may also provide other macro-elements (N, P) at defined stoichiometric ratios. These two factors need to be accounted for in model-based assessment of chemical persistence.

Glyphosate is the most widely applied herbicide worldwide[22] and is subject of public and scientific debate. Due to its widespread usage, much is known about its fate in the environment for a wide range of conditions in different matrices.[23–29] Different microorganisms have been isolated capable of using glyphosate as a source of C, N, and P and energy [24,30–35] but the macro-element relations have never been thoroughly evaluated. Glyphosate is known to be biodegraded via (at least) two pathways, namely the so-called sarcosine pathway and the aminomethylphosphonic acid (AMPA) pathway.[36–39] In the sarcosine pathway, the C-P bond is cleaved via sarcosine (N-methylglycine) and ortho-phosphate with subsequent complete mineralisation. Sarcosine was never released as metabolite in these experiments but microbial degradation pathways were commonly agreed to occur via this intermediate. However, recent abiotic experiments also showed that glyphosate may directly oxidize in the presence of birnessite to glycine without release of sarcosine.[40]

In the AMPA pathway, the C-N bond is cleaved producing AMPA and glyoxylate. AMPA is considered to be the dominating metabolite that accumulates and is frequently detected in soils treated with glyphosate and in adjacent surface waters and sediments.[24,41–43] Fortunately, the environmental fate of ^{13}C and ^{15}N co-labeled glyphosate in a water-sediment system (OECD 308) was studied recently for the first time,[38] and transfer to biomass and bioNER formation was examined by analysis of the dual label incorporation into amino acids hydrolyzed from microbial proteins. In parallel to these processes, also AMPA accumulated. This data set provides the unique opportunity to extend the MTB method combined with the 'unified model for biodegradation and sorption' to multi-element use and incomplete degradation even in multi-phase systems.

Therefore, the aim of the present study was to improve predictive capabilities of environmental fate models and to capture these phenomena and to exploit the unique ^{13}C and ^{15}N co-labeled glyphosate data for evaluating the developed combined modeling methods for optimized interpretation of OECD 308 test systems. We aimed at describing metabolite formation (AMPA) as well as energy gain and macro-element fluxes (C and N) into microbial biomass. In addition, we derived and evaluated hypotheses about the metabolite formation and shifts of the metabolic pathways, for example the limitation of microbial growth by other macro-elements than C, here N, which is not mineralized and may cause N overflow in microbial cells. Substrate consumption, formation of products and biomolecules, and distribution of labeled C and N were analyzed to assess metabolic fluxes and macro-element availability.

2 Materials and Methods

Experimental data. The authors of the co-labelled glyphosate environmental fate study[38] kindly provided us with their original experimental data for model evaluation. Briefly the analyses included $^{13}CO_2$, the extractable ^{13}C and ^{15}N fractions in water and sediment, non-extractable ^{13}C and ^{15}N fractions in sediment. Amino acids, hydrolyzed from the parent proteins, and their isotopic composition were analyzed in the living microbial biomass fraction of sediment and in the total amino acid pool of the sediment fraction (sum of amino acids in both living and dead biomass). BioNER were quantified from the amount of ^{13}C and ^{15}N in amino acids. Both glyphosate and its major metabolite AMPA were measured in water and sediment. A schematic overview of the experimental system is shown in Figure S2a (for more details see Wang et al.[38]).

Growth yields. Theoretical microbial growth yields[20],[21] were calculated for glyphosate degradation via the sarcosine and the AMPA pathways and served as input to the 'unified model for biodegradation and sorption'.[20] The yield, *Y*, defined as the biomass formed per mass of chemical consumed, was determined from the Gibbs free energy of the transformation reaction combined with knowledge of the chemical's structure and microbial growth processes.[20]

When the mineralization of a chemical requires many steps or is carried out by a multitude of bacterial strains, the assumption of single-step mineralization may no longer be valid.[44] The determination of partial growth yields requires the description of individual metabolic steps and the flux of macro-elements, energy and electrons within the system must be considered.[44] The MTB method can accommodate stepwise transformation by adapting two parameters, namely the number of electrons, n_{bio}, and of C atoms, n_C, that can be acquired by microorganisms in a transformation step. An adjusted MTB method is presented below, with description of partial growth yield determination.

The microbial growth yield is calculated from the anabolic and catabolic yields:

$$\frac{1}{Y} = \frac{1}{Y_{\text{cata}}} + \frac{1}{Y_{\text{ana}}} \quad (1)$$

The catabolic yield is determined from the energy of the redox reaction captured by the microorganisms:

$$Y_{\text{cata}} = \frac{n_{\text{bio}}\,\Delta G_r^{m\prime}}{n\;\Delta G_{\text{ATP}}^{obs}} \times Y_{\text{ATP}} \quad (2)$$

where *n* is the number of electrons transferred in the redox reaction and n_{bio} is the number of electrons from the redox reaction available to the bacterium for energy generation. Empirically, two

electrons are transferred for each C-H bond oxidized; n_{bio} thus corresponds to the number of C-H bonds present in the substrate minus the number of C-H bonds in the formed metabolite. $\Delta G_r^{m'}$ is the Gibbs free energy of the redox reaction at metabolic conditions (1 mmol L^{-1} chemical activity, 0.1 mol L^{-1} ionic strength and pH 7).[45] ΔG_{ATP}^{obs} is the observed Gibbs energy needed to synthesize adenosine triphosphate (ATP, approx. 80 kJ mol^{-1}) for typical conditions inside a microbial cell, calculated from a ΔG value of 31.8 kJ/mol[46] divided by the microbial efficiency of 40%,[47] Y_{ATP} is the biomass yield on ATP (default 5 g cell dw mol^{-1} ATP for non-sugar substrates).[47]

The anabolic yield (Y_{ana}^{C}) is determined from the amount of C in the substrate available for the synthesis of new biomass:

$$Y_{\mathrm{ana}}^{\mathrm{C}} = \frac{n_{\mathrm{C}}\, M_{\mathrm{C}}}{\sigma_{\mathrm{C}}} \tag{3}$$

n_C is the moles of C acquired by the microorganisms in the transformation [mol], M_C is the molar mass of C [g mol^{-1}], and σ_C is the fraction of C in the dry cell [g C_{cell} g^{-1} cell dw].

Furthermore, the anabolic yield can also be dependent on other limiting substrates such as N (Y_{ana}^{N}):

$$Y_{\mathrm{ana}}^{\mathrm{N}} = \frac{n_{\mathrm{N}}\, M_{\mathrm{N}}}{\sigma_{\mathrm{N}}} \tag{4}$$

where the subscript *N* refers to N. For a microbial cell stoichiometry of $C_5H_7O_2N$ ($n_{C,cell}$ = 5 mol C per mol cell), 1 mol cell is 113 g (labeled N and C 119 g/mol), σ_C is 0.531 g C_{cell} g^{-1} cell dw and σ_N is 0.124 g N_{cell} g^{-1} cell dw.[48]

Flux of carbon, nitrogen, energy and electrons. Glyphosate ($C_3H_8NO_5P$) is biodegraded via two pathways: (i) the sarcosine pathway and (ii) the AMPA pathway.[36–38] All three C atoms and the N atom can be incorporated into cellular biomass (Figure S1) or released as fully oxidized C in CO_2 and fully reduced N in ammonium (NH_4^+). The oxidation state of N in glyphosate is -3, corresponding to its oxidation state in ammonium and amines. The oxidation state of P in GLP is +3 as it is a phosphonate.[49] The average oxidation state of the C atoms in GLP is +2/3. Also, when the phosphonate is oxidized to orthophosphate (+5) two electrons are released and the C in sarcosine is reduced to an oxidation state of 0. In total, the complete mineralization of glyphosate releases 12 electrons (see SI S2 for details).

Sarcosine pathway. Glyphosate is initially transformed into equimolar amounts of sarcosine ($C_3H_7NO_2$) and orthophosphate through cleavage of the C-P bond by C-P lyase.[36] Sarcosine is immediately transformed into equimolar quantities of formaldehyde (CH_2O) and glycine ($C_2H_5NO_2$),

in which both labels were found. ^{13}C and ^{15}N co-labelled glycine is thus evidence for the sarcosine pathway.[36] Formaldehyde and glycine are either incorporated into biomass or oxidized to CO_2. The full mineralization of glyphosate via the sarcosine pathway can be formulated as:

$$\begin{aligned} C_3H_8NO_5P + H_2O &\leftrightharpoons C_3H_7NO_2 + H_3PO_4 \\ C_3H_7NO_2 + 0.5\ O_2 &\leftrightharpoons C_2H_5NO_2 + CH_2O \\ C_2H_5NO_2 + CH_2O + 2.5\ O_2 + H^+ &\leftrightharpoons 3\ CO_2 + 2H_2O + NH_4^+ \end{aligned} \quad (5)$$

AMPA pathway. Glyphosate is oxidized to glyoxylate ($CHOCOO^-$) and AMPA (CH_6NO_5P) through cleavage of the C-N bond by, e.g., glyphosate oxidoreductase.[36] The C in AMPA has an oxidation state of 0 while the C in glyoxylate has an oxidation state of +2. AMPA and glyoxylate can further be metabolized to biomass or CO_2. According to the results of the glyphosate turnover experiment[38], we assume that AMPA is an accumulating metabolite retaining N and P and only C in glyoxylate is mineralized. The reaction describing the degradation via the AMPA pathway takes the following form:

$$C_3H_8NO_5P + 1.5O_2 \leftrightharpoons CH_6NO_3P + 2CO_2 + H_2O \quad (6)$$

Partial growth yields, biomass, metabolites and CO_2 formation. The MTB approach also includes a C mass balance method to calculate the formation of bioNER.[20] A modified method capable of considering competing transformation pathways, leading to both CO_2 and accumulating metabolites, is presented below.

The moles of C in glyphosate degraded via the AMPA pathway results in the formation of Y^C_{AMPA} moles of biomass C per mol glyphosate C (mol C (mol C)$^{-1}$), n_{ox} moles of CO_2 per mol glyphosate C (mol C (mol C)$^{-1}$), and C_{AMPA} moles of C in AMPA (mol C):

$$C_{GLP} = \underbrace{Y^C_{AMPA} \times C_{GLP}}_{X\ \text{formed}} + \underbrace{n_{ox} \times C_{GLP}}_{CO_2\ \text{formed}} + \underbrace{C_{AMPA}}_{\text{AMPA formed}} \quad (7)$$

where C_{GLP} is moles of C in glyphosate. Normalizing with C_{GLP} gives (in units mol C (mol C)$^{-1}$):

$$1 = Y^C_{AMPA} + n_{ox} + \frac{C_{AMPA}}{C_{GLP}} = Y^C_{AMPA} + n_{ox} + \frac{1}{3} \quad (8)$$

Glyphosate degraded via the sarcosine pathway results in the formation of Y^C_{SRC} moles of biomass C and (1- Y^C_{SRC}) moles of CO_2 and the mass balance is simply:

$$C_{GLP} = \underbrace{Y^C_{SRC} \times C_{GLP}}_{X\ \text{formed}} + \underbrace{(1 - Y^C_{SRC}) \times C_{GLP}}_{CO_2\ \text{formed}} \quad (9)$$

One can calculate Y^{C}_{AMPA} and Y^{C}_{SRC} and the moles of glyphosate degraded via the AMPA pathway are measured (equal to the moles of AMPA formed), thus the total amount of biomass and CO_2 formed can be found from the sum of biomass and CO_2 formed via both pathways:

$$\text{Total } CO_2 = \underbrace{n_{ox} \times C^{AMPA}_{GLP}}_{\text{AMPA pathway}} + \underbrace{(1 - Y^{C}_{SRC}) \times C^{SAR}_{GLP}}_{\text{Sarcosine pathway}} \quad (10a)$$

$$\text{Total biomass} = \underbrace{Y^{C}_{AMPA} \times C^{AMPA}_{GLP}}_{\text{AMPA pathway}} + \underbrace{Y^{C}_{SRC} \times C^{SAR}_{GLP}}_{\text{Sarcosine pathway}} \quad (10b)$$

where C^{SAR}_{GLP} and C^{AMPA}_{GLP} denote the moles of glyphosate degraded via either pathway. The total amount of biomass includes both living and dead biomass, i.e., the bioNER formed.

Model structure. The test system was described as a multi-compartment model including mass transfer between water and sediment. Based on the experimental results, only glyphosate and AMPA were explicitly considered in the model, while other intermediates were assumed to be readily susceptible to biodegradation. State variables were: mass of glyphosate in supernatant water (*W*), pore water (*D*), sediment (*A*), sequestered (S); mass of AMPA in supernatant water, pore water, sediment; microbial biomass in sediment (*X*); mass of CO_2. The $^{13}C/^{15}N$ ratio of the NER was >3 (except at the final measurement), indicating that the amount of NER formed from AMPA (C/N equal to 1) was negligible and thus assumed to not occur.

The experimental system was unstirred, hence exchanges between compartments were controlled by diffusive transport.[3] Exchange between the supernatant water and the sediment pore water were described as diffusion through an unstirred boundary layer and to a sediment depth of 1 mm, based on the calculated depth of diffusion within 80 days[50] (see also SI S4) and penetration depth of O_2.[7] Biodegradation was assumed to occur only for glyphosate dissolved in the sediment pore water (*D*), as negligible formation of AMPA and CO_2 was observed in experiments containing only the creek water used in the experiment.[38] Exchange processes were described with well-established first-order kinetics,[11,20] hence, only the equations related to the biodegradation of glyphosate, microbial growth and formation of bioNER are presented in detail. Calculations were made in the unit µmol compound. All the model equations can be found in the SI S4, and all input data are listed in Table S5. A schematic overview of the model compartments is shown in Figure S2b. Seven model parameters together with the associated model uncertainty were estimated using the Bayesian optimization method DiffeRential Evolution Adaptive Metropolis algorithm (DREAM).[51] Details can be found in the SI S5.

Biodegradation of glyphosate. The experimental data show that glyphosate was a source of both N and C as ^{13}C and ^{15}N were incorporated into amino acids of proteins, and thus also into microbial biomass. The N/P ratio in microbial biomass is 13:1 on a molar basis,[52] while in glyphosate it is 1:1.

We can therefore safely assume that N is limiting anabolism before P, unless there are external N sources available.. The ratio of C/N in microbial biomass is 5:1, while it is 3:1 in glyphosate. Thus, once N and P supply is secured by degradation of glyphosate via the sarcosine pathway, only C is limiting microbial anabolism, also because a large fraction of C must be oxidized to CO_2 for the energy gain (catabolism). Degradation via the AMPA pathway does not provide N nor P for the degrader but it provides glyoxylate, an excellent C and energy source. Therefore, the observed shift in pathways, as indicated by the accumulation of AMPA, must be modulated by changes of the substrate needs. Filling the pools of N or P in the degrading microorganisms combined with energy limitations may signal the metabolic shift. In order to reflect the experimental results of the degradation through the AMPA pathway was thus modeled as a being dually limited, i.e. the respective transformation rate is dependent upon the N from the sarcosine pathway incorporated into the biomass and down-regulated as long as N is limiting. The metabolic fluxes for glyphosate degradation through the sarcosine and AMPA pathway are described using *Michaelis-Menten* kinetics:

$$\frac{\mathrm{d}n_{\mathrm{M,SRC}}}{\mathrm{d}t} = v_{\mathrm{max,SRC}} \frac{a_{\mathrm{D}}}{a_{\mathrm{D}} + K_{\mathrm{S,SRC}}} X \tag{11}$$

$$\frac{\mathrm{d}n_{\mathrm{M,AMPA}}}{\mathrm{d}t} = v_{\mathrm{max,AMPA}} \frac{a_{\mathrm{D}}}{a_{\mathrm{D}} + K_{\mathrm{S,AMPA}}} \frac{a_{\mathrm{D}}^{\mathrm{N}}}{a_{\mathrm{D}}^{\mathrm{N}} + K_{\mathrm{S}}^{\mathrm{N}}} X \tag{12}$$

where n_{M} [µmol] is the metabolized amount of glyphosate, X is the amount of degrader microbes [µmol bacteria], v_{max} [µmol (µmol bacteria d)$^{-1}$] is the maximum transformation rate and K_{S} [µmol L^{-1}] is the half-saturation constant for glyphosate through the sarcosine and AMPA pathway (subscript SRC and AMPA, respectively), and the N released from the sarcosine pathway (superscript N), a_{D} is the chemical activity of glyphosate or AMPA (equivalent to the freely dissolved concentration, µmol L^{-1}) in sediment pore water (index D). The chemical activity of dissolved inorganic N $a_{\mathrm{D}}^{\mathrm{N}}$ is calculated from the NH_4^+ released during mineralization of glyphosate through the sarcosine pathway resulting in potential turnover inhibition.

Biomass formation. Microbial growth was described by *Monod* kinetics including a term for microbial decay (similar to previous studies[11,53,54]):

$$\frac{\mathrm{d}X}{\mathrm{d}t} = Y_{\mathrm{SRC}} \times \frac{\mathrm{d}n_{\mathrm{M,SRC}}}{\mathrm{d}t} + Y_{\mathrm{AMPA}} \times \frac{\mathrm{d}n_{\mathrm{M,AMPA}}}{\mathrm{d}t} - b \times X \tag{13}$$

where the first two terms consider microbial growth and the last term considers microbial decay. Y_{SRC} and Y_{AMPA} [µmol bacteria (µmol substrate)$^{-1}$] are microbial growth yields of the sarcosine and

AMPA pathways, respectively, $dn_{M,SRC}/dt$ and $dn_{M,AMPA}/dt$ are the metabolic fluxes, and b [d^{-1}] is a first-order rate constant of microbial decay.

Microbial necromass, X_{necro} [µmol bacteria], is formed by the decay of living biomass X and is subject to slow mineralization with rate constant k_m [d^{-1}], here set to 0.001 d^{-1} comparable to that of soil organic matter:[11]

$$\frac{dX_{necro}}{dt} = b \times X - k_m \times X_{necro} \quad (14)$$

Living bacterial mass and necromass both contribute to the formation bioNER:

$$\frac{dbioNER}{dt} = \frac{dX}{dt} + \frac{dX_{necro}}{dt} \quad (15)$$

Microbial growth has been monitored by stable isotope incorporation into amino acids/proteins of living biomass.[16,17,19,38,55,56] To calculate the total label incorporation into other biomolecules than amino acids, a factor of 2 has usually been applied to calculate the biomass and bioNER resp., from measured amino acids (~50% of a dry cell is proteins[57]).[9]

Carbon dioxide. CO_2 was assumed to originate from the mineralization of glyphosate via both pathways and from microbial necromass:

$$\frac{dn_{CO_2}}{dt} = \left(1 - Y^C_{SRC}\right)\frac{dn_{M,SRC}}{dt} n_{C,SRC} + \left(1 - Y^C_{AMPA}\right)\frac{dn_{M,AMPA}}{dt} n_{C,AMPA} + k_m X_{necro} n_{C,cell} \quad (16)$$

These calculations refer to a C basis: n_{CO2} [µmol] is the amount of formed CO_2. Three moles C are metabolized via the sarcosine pathway (with $n_{C,SRC}$ is 3 mol C per mol glyphosate) and only two moles C via the AMPA pathway (with $n_{C,AMPA}$ is 2 mol C per mol glyphosate), since AMPA accumulates. Y^C_{SRC} and Y^C_{AMPA} are microbial growth yields (moles of C in bacteria per moles of C in substrate, or g C g^{-1} C).[20]

3 Results

Microbial growth yield estimates of glyphosate degradation. Table 1 shows the calculated microbial growth yields and thermodynamic analysis of the different pathways. Negative $\Delta G_r^{m'}$ values indicate exothermic, energetically favorable, reactions. The first step of the sarcosine pathway (glyphosate → sarcosine) is favorable, while the first step of the AMPA pathway (glyphosate → AMPA + glyoxylate) is not. If glyoxylate mineralization is included, the reaction is thermodynamically favorable. $\Delta G_r^{m'}$ of the mineralization via the sarcosine pathway is more than six-fold that of the incomplete AMPA pathway, which is also reflected in the estimated growth yields. The difference between Y^C_{ana} and Y^N_{ana} shows that glyphosate is a better source of N than

of C for microbial growth, indicating that C is the limiting substrate. For the sarcosine pathway, the majority of the microbial yield is associated to metabolism of glycine and formaldehyde. The anabolic contribution is higher than the catabolic contribution ($Y^{C}_{ana} > Y_{cata}$). In the AMPA pathway, most of the potential energy and the N mass are retained in AMPA. If AMPA is an accumulating metabolite (as seen in this study), then only glyoxylate metabolism provides C and energy. However, the question remains open why AMPA is not degraded under the test conditions, although its mineralization seems very energetically favorable, see discussion.

Table 1. Estimated microbial growth yields of the different degradation steps in the sarcosine and AMPA pathways.

	$\Delta G_r^{m\prime}$	n_{bio}/n	C-H bonds cleaved	Y^N_{ana}	Y^C_{ana}	Y_{cata}	Y^C	Y^C
	kJ mol^{-1}			g bac mol^{-1}	g bac mol^{-1}	g bac mol^{-1}	g bac mol^{-1}	g C g^{-1} C
Sarcosine pathway								
Glyphosate -> sarcosine + P_i	−90	0/0	0	0	0	0	0	0
Sarcosine -> glycine + formaldehyde	−182	2/2	1	0	0	11.4	0	0
Glycine -> 2 CO_2	−708	4/6	2	119	47.6	29.5	18.2	0.38
Formaldehyde -> CO_2	−500	4/4	2	0	23.8	31.2	13.5	0.57
AMPA pathway								
Glyphosate -> AMPA + glyoxylate	*247*	2/2	1	0	0	*<0*	0	0
AMPA -> CO_2	−1211	4/6	2	119	23.8	50.5	16.2	0.68
Glyoxylate -> 2 CO_2	−515	2/4	1	0	47.6	16.1	12.0	0.25
Used for calculation								
Glyphosate -> 3 CO_2	−1480	8/12	4	119	71.4	61.7	33.1	0.46
Glyphosate -> AMPA + 2 CO_2	−268	4/6	2	0	47.6	11.2	9.1	0.19

The calculations were done for metabolic conditions (superscript m: for chemical activities of 0.1 mmol L^{-1} and ionic strength of 0.1 mol L^{-1}) and pH is 7 (superscript ‘). $\Delta G_r^{m\prime}$ is the Gibbs energy of the redox reaction (kJ mol^{-1}), Y^C_{ana} is the anabolic yield on C in the substrate, Y^N_{ana} is the anabolic yield on N in the substrate, Y_{cata} is the catabolic yield gained from the redox reaction, Y^C is the microbial growth yield if C is the limiting substrate and is calculated from Y_{cata} and Y^C_{ana}. Unit is g bacteria dry weight per mol substrate, except the last column in mol C in bacteria per mol C substrate (g C g^{-1} C). 1 mol bacteria is 119 g (^{13}C and ^{15}N labeled).

Model results, uncertainty and parameter identifiability. The seven calibrated input parameters and their quality criteria (credibility interval, coefficient of variation σ/μ, maximum absolute correlation coefficient *r*) are shown in Table 2. Only $X(0)$ and $K_{OC,GLP}$ can be considered identifiable based on the criteria by Frutiger et al.[58] (r < 0.7, CV = σ/μ < 0.5), due to the high positive correlation between the v_{max}-values and their accompanying K_S-values.

Table 2: Result of the DREAM parameter optimization. The set of parameters resulting in the maximum a-posterior probability are listed together with their 95% credibility interval (CI), the coefficient of variation CV (σ/μ) and the maximum absolute correlation coefficient (abs r (max)).

Parameter	Unit	Optimum (95% CI)	CV	abs *r* (max)
$v_{max,SRC}$	μmol glyphosate (μmol bacteria d)$^{-1}$	2.56 (0.47; 3.45)	0.39	0.87
$K_{S,SRC}$	μmol glyphosate L^{-1}	391 (52.0; 395)	0.35	0.87
$K_{OC,GLP}$	L kg$_{OC}^{-1}$	882 (769;1093)	0.09	0.28
$v_{max,AMPA}$	μmol glyphosate (μmol bacteria d)$^{-1}$	26.9 (8.71; 29.6)	0.30	0.89
$K_{S,AMPA}$	μmol glyphosate L^{-1}	1327 (431; 1484)	0.29	0.89
$K_{S,N}$	μmol glyphosate L^{-1}	47.0 (3.34; 76.9)	0.56	0.50
X(0)	μmol bacteria L^{-1}	0.050 (0.021; 0.13)	0.45	0.55

Simulation results for both ^{13}C and ^{15}N are shown and compared to experimental data in Figure 1. The degradation of glyphosate, formation of AMPA, formation of NER, and formation of CO_2 are captured very well (RMSE 2.2). Simulated ^{13}C in bioNER was lower than the ^{13}C-total amino acids until day 40, while simulated ^{15}N in bioNER was strikingly lower than the ^{15}N-total amino acids measured at all times. Obviously, ^{13}C and ^{15}N were not incorporated into biomass in the expected C/N ratio of 5:1. The initial difference between bioNER and total NER is three times higher on a ^{13}C basis than on a ^{15}N basis (Figure 1b,d), and it is likely that it is sequestered glyphosate. In addition, measured ^{15}N in total amino acids is much higher than the simulated bioNER, indicating that N is intermediately enriched in the biomass and not released as NH_4^+, thus N is presumably the control factor. Remarkably, the use of the simple modified carbon mass balance gives in general similar final values for bioNER (total biomass) and CO_2 (shown as arrows in Figure 1a,b).

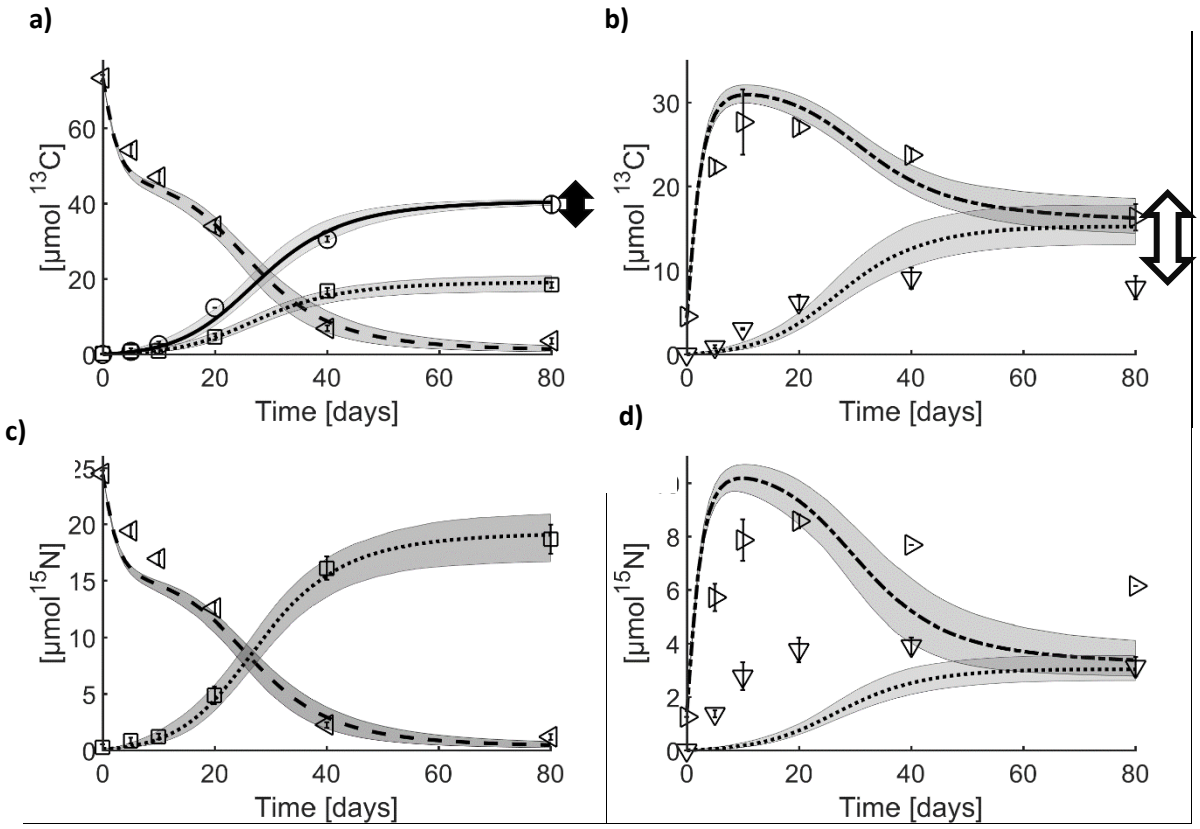

Figure 1. Model simulations using the optimized parameter set determined using DREAM. Results shown in µmol ^{13}C (a,b) and µmol ^{15}N (c,d). Lines are model simulations and symbols are measurements. Vertical bars indicate the standard deviation of the measurements. **(a,c)** Extractable fractions of glyphosate (−−; ◁), AMPA (▪▪; □) and CO_2 (**−**; ○); **(b,d)** Formation of simulated and measured total NER (−-; ▷), measured total amino acids (▽) and simulated bioNER (**...**). The grey bands delineate the 95% credibility interval of the model simulations. The vertical arrows in panels (a) and (b) show the upper and lower bounds of the formed amounts of CO_2 (black) and bioNER (white) calculated using the modified MTB carbon balance method (see SI S8 for details).

$^{13}C/^{15}N$-ratio. Co-labeling with ^{13}C and ^{15}N allowed calculating observed $^{13}C/^{15}N$ ratios in amino acids and NER over the duration of the experiment. The measured $^{13}C/^{15}N$ ratios in total amino acids, NER, and amino acids in living cells are shown in Figure 2 together with the formation of AMPA. The $^{13}C/^{15}N$ ratios in amino acids in living cells and total amino acids were initially <1, with the ratio in amino acids in living cells converging to approximately 1 at the end of the experiment. The $^{13}C/^{15}N$-ratio in total amino acids increased concomitantly with the formation of AMPA to a maximum of 2.6, while the average C/N ratio of amino acids in living cells is 3.7:1 (Table S2). This

shows that ^{15}N was initially incorporated into amino acids to a larger extent than ^{13}C. As glyphosate is an aminophosphonic acid analog of glycine, it is not surprising that ^{13}C and ^{15}N were predominately found in glycine (60% of the ^{13}C and 34% of the ^{15}N measured in total amino acids on day 5).[38] The Y^C for the sarcosine pathway (Table 1) is 0.46, i.e. 54% of C forms CO_2 if glyphosate is the sole C source. However, the measured $^{13}CO_2/^{13}C$-total amino acids ratio was <1 until day 20 (Fig. 2). After day 20, when the AMPA pathway dominates, only ^{13}C was incorporated in amino acids, and the $^{13}C/^{15}N$-ratio in total amino acids rose above 1. In the NER, the $^{13}C/^{15}N$-ratio was >3 in all measurements except the last (80 days). At the end of the experiment, the $^{13}C/^{15}N$ ratios in NER and in total amino acids were similar, suggesting that the NER are predominately biogenic, which is supported by the model simulations. Therefore, the modeling approach reflecting the experimental data conclusively shows that C is limiting or the excess of N is triggering the shift from sarcosine pathway towards AMPA formation.

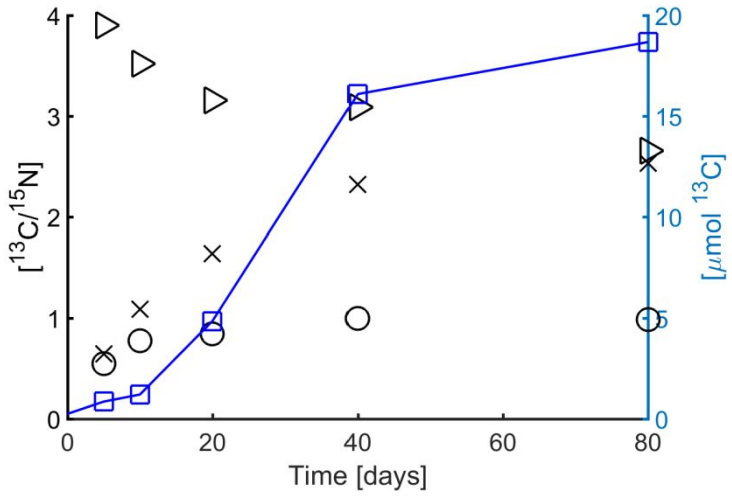

Figure 2. $^{13}C/^{15}N$ ratio measured in the experiment. Left axis: $^{13}C/^{15}N$ ratio in the measured total amino acids (×), living amino acids (○), and non-extractable residues (NER) (▷) over time. Right axis (blue): Measured AMPA in μmol (-□-).

4 Discussion

The primary goal of the present study was to extend and validate the microbial growth yield estimation (MTB) method combined with the 'unified model for biodegradation and sorption' in order to capture the phenomena of various transformation pathways with metabolite formation and multi-substrate use for optimized interpretation of OECD 308 (and also 307) test systems. This was performed for a ^{13}C and ^{15}N co-labeled glyphosate degradation experiment[38]. Glyphosate consumption, formation of metabolites (AMPA) and biomolecules, as well as energy gain and distribution of ^{13}C and ^{15}N were successfully modeled and the metabolic fluxes and element availability were assessed. Anabolic yield calculations conditioned on the microbial C and N demands gave insights into nutrient limitations and were confirmed by the measured $^{13}C/^{15}N$ ratios. The results showed that glyphosate mineralization via the sarcosine pathway gave a higher growth yield than via the (incomplete) AMPA pathway. However, in a later stage of degradation the release of AMPA may protect the cells from N overflow which may cause the accumulation of this transformation product. The extended modeling methods allow improved interpretations and hypothesis derivation for transformation pathways in environmental fate test systems by considering the bioenergetic feasibility and influential factors, such as nutrient limitation and element distribution.

Model performance. The model simulations were able to fully capture the experimental elimination of glyphosate and the concurrent formation of total NER, AMPA and CO_2 observed in the OECD 308 setup. However, the formation of biomass as observed by amino acid analysis was only partly reflected. This is caused by the analytical bias introduced when biomass formation is calculated from amino acid analysis of hydrolyzed microbial proteins (SI S3). While other model structures[3,6,8] have been used to capture the dynamics of the OECD 308 test system and formation of NER they do not provide any information regarding the biomass formation, NER composition, and macro-element distribution. The prediction of the NER composition, in particular the bioNER contribution, requires the mechanistic description of microbial growth and decay in the model.

The calibration procedure resulted in acceptable uncertainty ranges of the estimated parameters and model output (Table 2 and Figure 1). The maximum specific growth rate found for the AMPA pathway ($\mu_{max,\ AMPA}$ 2.04 d^{-1}) is comparable to previously reported findings, while, the one determined for the sarcosine pathway ($\mu_{max,\ SRC}$ 0.71 d^{-1}) is lower.[36] However, direct comparison is difficult due to the difference in the measurement units reported. The determined affinity constant $K_{S,SRC}$ (391 µmol L^{-1}) is higher than the ranges reported for *Pseudomonas* sp. strain PG2982 (23 µmol L^{-1}) and *Arthrobacter* spp. (105–125 µmol L^{-1}).[32,59] For soil microcosms the value was estimated to be 412–4050 µmol L^{-1}.[60] The value obtained for $K_{S,N}$ is within the affinity data compiled for ammonia elsewhere.[61]

Shift of transformation pathways. From a thermodynamic perspective, the sarcosine pathway is preferable to the AMPA pathway (Table 1) and gives access to the nutrients N and P, although in an over-stoichiometric relation in comparison to microbial biomass. However, the experimental data show that microorganisms favored the AMPA pathway after day 10. Based on the macro-element availability in glyphosate, we hypothesized that P is in surplus in this molecule and that N saturation and C deficit modulated the switch of pathways leading to the formation of AMPA. The calculated Y^{N}_{ana} is 1.7 times higher than Y^{C}_{ana}, further indicating that C is limiting the anabolism. Microorganisms thus need to support their growth by using other C sources than glyphosate, since the glyphosate degradation via the sarcosine pathway forms CO_2 resulting in NH_4^+ release and overflow in the living cells. Once sufficient N is available from the sarcosine pathway due to C mineralisation, the faster formation of AMPA dominates and prevents the cells from internal ammonia-N overflow. This may be an explanation for the AMPA accumulation under the batch conditions of the OECD test 308 and other batch test systems and also explain AMPA occurrence in the environment due to slower AMPA turnover.[62] Similar results were found for glyphosate in OECD 307 fate studies in soil but with lower amounts of microbial biomass.[63] Also, the sarcosine pathway is more costly in terms of enzyme synthesis (C-P lyase), which may cause slower substrate turnover and growth of microorganisms than the AMPA pathway (see v_{max} and μ_{max} values, Table 2 and Table S5).

The $^{13}C/^{15}N$ ratio measured in amino acids is much lower than 3:1 (in glyphosate) until day 40, which indicates the use of non-glyphosate C sources for anabolism and challenges the assumption of single substrate use and stable isotope probing approaches in general.[64] Under the batch conditions of OECD 308 test, but presumably also in soils (OECD 307), the initial mixing and rewetting of the sediment can make organic matter available as substrate and lead to an initial burst of (non-labeled) CO_2 (Birch effect).[65] When this initial effect is gone, starvation will prevail and may also trigger a shift in the glyphosate degradation pathways, particularly under C limitations. The use of other C sources without a considerable impact on catabolism or anabolism may be explained by the mining of microbial building blocks by the degrader microorganisms with minimal energetic impact on the anabolism. These building blocks can be derived from microbial necromass always present in sediments and soils. Additional C sources have consequences for the amount of living biomass when calibrated to measured amino acids, and for the fitted maximum rate ($v_{max} \cdot X$). We therefore excluded the measurements of amino acids hydrolyzed from proteins in the model calibration. However, these were used to assess biomass and bioNER formation. In SI S3, theoretically sound conversion factors are derived to convert measurements of ^{13}C- or ^{15}N-amino acids into total biomass. "Apparent" conversion factors can be calculated by dividing the simulated ^{13}C- or ^{15}N-bacterial biomass with the measured ^{13}C- or ^{15}N-total amino acids (Figure 1).

The "apparent" conversion factors not only varied in time, they were also much lower than the theoretical factors for glyphosate as sole substrate derived in SI S3 and the commonly applied factor of 2.[12] For N, the apparent factor was as low as 0.16 and increased to 0.97 by the end of the experiment. For C it increased from 0.33 to 1.9. This further indicates that N is predominately used in amino acid synthesis and is stored within the cells whereas C is not. Consequently, the theoretical conversion factors and the commonly applied factor of 2 are not valid under the observed conditions. Consequently, the use of these leads to the overestimation of bioNER early in the simulation test.

Hypothetically, the shift in transformation pathways could be caused by both N and P releases. Low intracellular orthophosphate (P_i) concentrations have been shown to enhance the activity of the enzymatic complex (C-P lyase) of the sarcosine pathway while high concentrations are inhibitory .[35,37] The maximum concentration of P_i in the top 1 mm pore water (= boundary layer, assuming that 90% of all glyphosate-P_i is released)[59] and overlying water is 78 µmol L^{-1}, which is similar to the inhibition coefficients (K_i) reported (24–253 µmol L^{-1}) and may explain the inhibition of the sarcosine pathway.[31,60] The concentration is however much lower than the inhibition coefficient reported for the mutant strain GLP-1/Nit-1 (2,300 µmol L^{-1}).[31] In addition, P_i competes with glyphosate for sorption sites, indicating that it does not remain in solution[66] and thus the P inhibition hypothesis in the present experiments appears unlikely. This hypothesis together with the hypothesis that AMPA is degraded has been tested using the model and further information can be found in SI S6. In Lake Greifensee in Switzerland, the concentration of both glyphosate and AMPA was observed to decline concomitantly with the depletion of P_i and a bloom of cyanobacteria.[42] Cyanobacteria are photoautotrophs, hence, unaffected by the lack of an organic C source. As some species are also capable of fixing atmospheric N, it is likely that the disappearance of AMPA and glyphosate in such lakes is driven by a need for P.

Considering the C limitation and the less likely impact of P inhibition, N can be identified as the trigger factor of the shift of degradation pathways to AMPA accumulation. Via the sarcosine pathway, C is mineralized and eliminated whereas N is not. As shown by the experimental data, NH_4^+ obviously remains in the degrader cells thus leading to an N overflow within the cells. Thus, it is justified to hypothesize that the accumulation of AMPA provides a solution to discard excess N and P and at the same time provide glyoxylate as a C and energy source.

Relevance and research needs. The ‘unified model for biodegradation and sorption’ combined with the extended MTB approach provides a powerful tool for the simulation of biodegradation and bioNER formation, even in complex experimental settings and with multiple pathways and macro-element availability. We could show that the developed modeling approach was able to capture

water-sediment mass transfer as well as turnover of real experimental data based on yield estimates for incomplete metabolism. When combined with experiments with multiple isotope labels in a single substrate,[38] the anabolic yield calculations gave valuable additional insights, in particular when compared to measured ^{15}N and ^{13}C labels, and provided the unique opportunity to derive hypotheses to explain the shift of microbial degradation and metabolite formation pathways. The results show that glyphosate degradation is C limited and increasing internal overflow of ammonia in degrader cells, presumably combined with starvation of the C turnover under the test conditions, may cause the accumulation of AMPA. One may speculate that in order to avoid AMPA accumulation when using glyphosate, application of fertilizer and N-rich manure should be applied only when easily assimilable C sources are available or should be supplied much later than glyphosate application. Future studies should therefore investigate factors determining the accumulation of AMPA (being a potential nutritious substrate) for mitigating its occurrence as a widely observed accumulating metabolite of a generally biodegradable herbicide.

Supporting Information

Data for the calculation of the microbial growth yields; half-reactions describing the transformation pathways; equations and tables showing how the factors for converting C and N amounts in amino acids to C and N amounts in bacterial cells were derived; equations for the model implementation; detailed results of the DREAM parameter inference method; C and N balances.

Acknowledgements

This collaborative research was financed by general institutional research funds of DTU, UFZ and TUM. We thank the unknown reviewers for their comments and the resulting improvement of the manuscript.

References

(1) European Commission. *Regulation (EC) No 1907/2006 - Registration, Evaluation, Authorisation and Restriction of Chemicals (REACH)*; 2006.

(2) OECD. *Test No. 307: Aerobic and Anaerobic Transformation in Soil*; Paris, 2002.

(3) Honti, M.; Fenner, K. Deriving Persistence Indicators from Regulatory Water-Sediment Studies - Opportunities and Limitations in OECD 308 Data. *Environ. Sci. Technol.* **2015**, *49* (10), 5879–5886.

(4) European Commission. *Regulation (EC) No 1107/2009 of the European Parliament and of the Council of 21 October 2009 Concerning the Placing of Plant Protection Products on the Market*; 2009.

(5) ECHA. *Guidance on Information Requirements and Chmical Safety Assessment. Chapter R.11: PBT/VPvB Assessment (Version 3.0)*; Helsinki, Finland, 2017.

(6) Honti, M.; Hahn, S.; Hennecke, D.; Junker, T.; Shrestha, P.; Fenner, K. Bridging across OECD 308 and 309 Data in Search of a Robust Biotransformation Indicator. *Environ. Sci. Technol.* **2016**, acs.est.6b01097.

(7) Shrestha, P.; Junker, T.; Fenner, K.; Hahn, S.; Honti, M.; Bakkour, R.; Diaz, C.; Hennecke, D. Simulation Studies to Explore Biodegradation in Water–Sediment Systems: From OECD 308 to OECD 309. *Environ. Sci. Technol.* **2016**, *50* (13), 6856–6864.

(8) Ter Horst, M. M. S.; Koelmans, A. A. Analyzing the Limitations and the Applicability Domain of Water-Sediment Transformation Tests like OECD 308. *Environ. Sci. Technol.* **2016**, *50* (19), 10335–10342.

(9) Kästner, M.; Trapp, S.; Schäffer, A. Consultancy Services to Support ECHA in Improving the Interpretation of Non-Extractable Residues (NER) in Degradation Assessment. Discussion Paper - Final Report. Edited by the European Chemical Agency ECHA (June 2018), available at www.echa.europa.eu/publications/technical-scientific-reports.

(10) Barriuso, E.; Benoit, P.; Dubus, I. G. Formation of Pesticide Nonextractable (Bound) Residues in Soil: Magnitude, Controlling Factors and Reversibility. *Environ. Sci. Technol.* **2008**, *42* (6), 1845–1854.

(11) Kästner, M.; Nowak, K. M.; Miltner, A.; Trapp, S.; Schäffer, A. Classification and Modelling of Nonextractable Residue (NER) Formation of Xenobiotics in Soil – A Synthesis. *Crit. Rev. Environ. Sci. Technol.* **2014**, *44* (19), 2107–2171.

(12) Schäffer, A.; Kästner, M.; Trapp, S. A Unified Approach for Including Non-Extractable Residues (NER) of Chemicals and Pesticides in the Assessment of Persistence. *Environ. Sci. Eur.* **2018**, *30*, 1–14.

(13) Barraclough, D.; Kearney, T.; Croxford, A. Bound Residues: Environmental Solution or Future Problem? *Environ. Pollut.* **2005**, *133* (1), 85–90.

(14) ECETOC. *Technical Report No. 118 - Development of Interim Guidance for the Inclusion of Non-Extractable Residues (NER) in the Risk Assessment of Chemicals*; Brussels, Belgium, 2013.

(15) Roberts, T.; Klein, W.; Stillm, G.; Kearney, P.; Drescher, N.; Desmoras, J.; Esser, H.; Aharonson, N.; Vonk, J. Non-Extractable Pesticide Residues in Soils and Plants. *Pure Appl. Chem.* **1984**, *56* (7), 945–956.

(16) Nowak, K. M.; Miltner, A.; Gehre, M.; Schäffer, A.; Kastner, M. Formation and Fate of Bound Residues from Microbial Biomass during 2, 4-D Degradation in Soil. *Environ. Sci. Technol.* **2011**, *45* (3), 999–1006.

(17) Nowak, K. M.; Girardi, C.; Miltner, A.; Gehre, M.; Schäffer, A.; Kästner, M. Contribution of Microorganisms to Non-Extractable Residue Formation during Biodegradation of Ibuprofen in Soil. *Sci. Total Environ.* **2013**, *445–446*, 377–384.

(18) Kästner, M.; Nowak, K. M.; Miltner, A.; Schäffer, A. (Multiple) Isotope Probing Approaches to Trace the Fate of Environmental Chemicals and the Formation of Non-Extractable “bound” Residues. *Curr. Opin. Biotechnol.* **2016**, *41*, 73–82.

(19) Poßberg, C.; Schmidt, B.; Nowak, K.; Telscher, M.; Lagojda, A.; Schaeffer, A. Quantitative Identification of Biogenic Nonextractable Pesticide Residues in Soil by 14C-Analysis.

Environ. Sci. Technol. **2016**, *50* (12), 6415–6422.
(20) Trapp, S.; Brock, A. L.; Nowak, K.; Kästner, M. Prediction of the Formation of Biogenic Nonextractable Residues during Degradation of Environmental Chemicals from Biomass Yields. *Environ. Sci. Technol.* **2018**, *52* (2), 663–672.
(21) Brock, A. L.; Kästner, M.; Trapp, S. Microbial Growth Yield Estimates from Thermodynamics and Its Importance for Degradation of Pesticides and Formation of Biogenic Non-Extractable Residues. *SAR QSAR Environ. Res.* **2017**, *28* (8), 629–650.
(22) Benbrook, C. M. Trends in Glyphosate Herbicide Use in the United States and Globally. *Environ. Sci. Eur.* **2016**, *28* (1), 1–15.
(23) Barja, B. C.; Dos Santos Afonso, M. Aminomethylphosphonic Acid and Glyphosate Adsorption onto Goethite: A Comparative Study. *Environ. Sci. Technol.* **2005**, *39* (2), 585–592.
(24) Borggaard, O. K.; Gimsing, A. L. Fate of Glyphosate in Soil and the Possibility of Leaching to Ground and Surface Waters: A Review. *Pest Manag. Sci.* **2008**, *64* (4), 441–456.
(25) Simonsen, L.; Fomsgaard, I. S.; Svensmark, B.; Spliid, N. H. Fate and Availability of Glyphosate and AMPA in Agricultural Soil. *J. Environ. Sci. Health. B.* **2008**, *43* (5), 365–375.
(26) Al-Rajab, A. J.; Amellal, S.; Schiavon, M. Sorption and Leaching of 14C-Glyphosate in Agricultural Soils. *Agron. Sustain. Dev.* **2008**, *28* (3), 419–428.
(27) Bento, C. P. M.; Yang, X.; Gort, G.; Xue, S.; van Dam, R.; Zomer, P.; Mol, H. G. J.; Ritsema, C. J.; Geissen, V. Persistence of Glyphosate and Aminomethylphosphonic Acid in Loess Soil under Different Combinations of Temperature, Soil Moisture and Light/Darkness. *Sci. Total Environ.* **2016**, *572*, 301–311.
(28) Nguyen, D. B.; Rose, M. T.; Rose, T. J.; Morris, S. G.; van Zwieten, L. Impact of Glyphosate on Soil Microbial Biomass and Respiration: A Meta-Analysis. *Soil Biol. Biochem.* **2016**, *92*, 50–57.
(29) Grandcoin, A.; Piel, S.; Baures, E. AminoMethylPhosphonic Acid (AMPA) in Natural Waters: Its Sources, Behavior and Environmental Fate. *Water Res.* **2017**, *117*, 187–197.
(30) Pipke, R.; Amrhein, N.; Jacob, G. S.; Schaefer, J.; Kishore, G. M. Metabolism of Glyphosate in an Arthrobacter-Sp Glp-1. *Eur. J. Biochem.* **1987**, *165*, 267–273.
(31) Pipke, R.; Amrhein, N. Degradation of the Phosphonate Herbicide Glyphosate By Arthrobacter-Atrocyaneus Atcc-13752. *Appl. Environ. Microbiol.* **1988**, *54* (5), 1293–1296.
(32) Fitzgibbon, J.; Braymer, H. D. Phosphate Starvation Induces Uptake of Glyphosate by Pseudomonas Sp. Strain PG2982. *Appl. Environ. Microbiol.* **1988**, *54* (7), 1886–1888.
(33) McAuliffe, K. S.; Hallas, L. E.; Kulpa, C. F. Glyphosate Degradation by Agrobacterium Radiobacter Isolated from Activated Sludge. *J. Ind. Microbiol.* **1990**, *6* (3), 219–221.
(34) Klimek, M.; Lejczak, B.; Kafarski, P.; Forlani, G. Metabolism of the Phosphonate Herbicide Glyphosate by a Non-Nitrate-Utilizing Strain of Penicillium Chrysogenum. *Pest Manag. Sci.* **2001**, *57* (9), 815–821.
(35) Sviridov, A. V.; Shushkova, T. V.; Ermakova, I. T.; Ivanova, E. V.; Epiktetov, D. O.; Leontievsky, A. A. Microbial Degradation of Glyphosate Herbicides (Review). *Appl. Biochem. Microbiol.* **2015**, *51* (2), 188–195.
(36) Sviridov, A. V.; Shushkova, T. V.; Zelenkova, N. F.; Vinokurova, N. G.; Morgunov, I. G.; Ermakova, I. T.; Leontievsky, A. A. Distribution of Glyphosate and Methylphosphonate Catabolism Systems in Soil Bacteria Ochrobactrum Anthropi and Achromobacter Sp. *Appl. Microbiol. Biotechnol.* **2012**, *93* (2), 787–796.
(37) Hove-Jensen, B.; Zechel, D. L.; Jochimsen, B. Utilization of Glyphosate as Phosphate Source: Biochemistry and Genetics of Bacterial Carbon-Phosphorus Lyase. *Microbiol. Mol. Biol. Rev.* **2014**, *78* (1), 176–197.
(38) Wang, S.; Seiwert, B.; Kästner, M.; Miltner, A.; Schäffer, A.; Reemtsma, T.; Yang, Q.; Nowak, K. M. (Bio)Degradation of Glyphosate in Water-Sediment Microcosms - A Stable Isotope Co-Labeling Approach. *Water Res.* **2016**, *99*, 91–100.
(39) Zhan, H.; Feng, Y.; Fan, X.; Chen, S. Recent Advances in Glyphosate Biodegradation Glyphosate. **2018**.

(40) Li, H.; Wallace, A. F.; Sun, M.; Reardon, P. N.; Jaisi, D. P. Degradation of Glyphosate by Mn–oxide May Bypass Sarcosine and Form Glycine Directly after C–N Bond Cleavage. *Environ. Sci. Technol.* **2018**, acs.est.7b03692.

(41) Aparicio, V. C.; De Gerónimo, E.; Marino, D.; Primost, J.; Carriquiriborde, P.; Costa, J. L. Environmental Fate of Glyphosate and Aminomethylphosphonic Acid in Surface Waters and Soil of Agricultural Basins. *Chemosphere* **2013**, *93* (9), 1866–1873.

(42) Huntscha, S.; Stravs, M. A.; Bühlmann, A.; Ahrens, C. H.; Frey, J. E.; Pomati, F.; Hollender, J.; Buerge, I. J.; Balmer, M. E.; Poiger, T. Seasonal Dynamics of Glyphosate and AMPA in Lake Greifensee: Rapid Microbial Degradation in the Epilimnion During Summer. *Environ. Sci. Technol.* **2018**, acs.est.8b00314.

(43) Silva, V.; Montanarella, L.; Jones, A.; Fernández-Ugalde, O.; Mol, H. G. J.; Ritsema, C. J.; Geissen, V. Distribution of Glyphosate and Aminomethylphosphonic Acid (AMPA) in Agricultural Topsoils of the European Union. *Sci. Total Environ.* **2018**, *621*, 1352–1359.

(44) VanBriesen, J. M.; Rittmann, B. E. Mathematical Description of Microbiological Reactions Involving Intermediates (Vol 67, Pg 35, 1999). *Biotechnol. Bioeng.* **2000**, *68* (6), 705.

(45) Flamholz, A.; Noor, E.; Bar-Even, A.; Milo, R. EQuilibrator - The Biochemical Thermodynamics Calculator. *Nucleic Acids Res.* **2012**, *40* (D1), 770–775.

(46) Thauer, R. K.; Jungermann, K.; Decker, K. Energy Conservation in Chemotrophic Anaerobic Bacteria. *Bacteriol. Rev.* **1977**, *41* (1), 100–180.

(47) Diekert, G. Grundmechanismen Des Stoffwechsels Und Der Energiegewinnung. In *Umweltbiotechnologie*; Ottow, J. C. G., Bidlingmaier, W., Eds.; Fischer Verlag: Stuttgart, Germany, 1997; pp 1–38.

(48) Christensen, D. R.; McCarty, P. L. Multi-Process Biological Treatment Model. *J. (Water Pollut. Control Fed.* **1975**, *47* (11), 2652–2664.

(49) LaRowe, D. E.; Van Cappellen, P. Degradation of Natural Organic Matter: A Thermodynamic Analysis. *Geochim. Cosmochim. Acta* **2011**, *75* (8), 2030–2042.

(50) FOCUS. Guidance Document on Estimating Persistence and Degradation Kinetics from Environmental Fate Studies on Pesticides in EU Registration. *Report of the FOCUS Work Group on Degradation Kinetics, EC Sanco/10058/2005*. 2006, pp 1–434.

(51) Vrugt, J. A. Markov Chain Monte Carlo Simulation Using the DREAM Software Package: Theory, Concepts, and MATLAB Implementation. *Environ. Model. Softw.* **2016**, *75*, 273–316.

(52) Tchobanoglous, G.; Burton, F.; Stensel, H. *Wastewater Engineering - Treatment and Reuse*, 4th ed.; McGraw-Hill, New York, US., 2003.

(53) Adam, I. K.; Rein, A.; Miltner, A.; da Costa, F. A.; Trapp, S.; Kaestner, M. Experimental Results and Integrated Modelling of Bacterial Growth on Insoluble Hydrophobic Substrate (Phenanthrene). *Env. Sci Technol* **2014**, *48*, 8717–8726.

(54) Rein, A.; Adam, I. K. U.; Miltner, A.; Brumme, K.; Kästner, M.; Trapp, S. Impact of Bacterial Activity on Turnover of Insoluble Hydrophobic Substrates (Phenanthrene and Pyrene)-Model Simulations for Prediction of Bioremediation Success. *J. Hazard. Mater.* **2016**, *306*, 105–114.

(55) Wang, S.; Miltner, A.; Nowak, K. M. Identification of Degradation Routes of Metamitron in Soil Microcosms Using 13C-Isotope Labeling. *Environ. Pollut.* **2017**, *220*, 927–935.

(56) Wang, S.; Miltner, A.; Kästner, M.; Schäffer, A.; Nowak, K. M. Transformation of Metamitron in Water-Sediment Systems_ Detailed Insight into the Biodegradation Processes. *Sci. Total Environ.* **2017**, *578*, 100–108.

(57) Madigan, M. T., Martinko, J. M., Bender, K. S., Buckley, D. H., & Stahl, D. A. *Brock Biology of Microorganisms*, 14th ed.; Pearson Inc.: Boston, USA, 2014.

(58) Frutiger, J.; Marcarie, C.; Abildskov, J.; Sin, G. A Comprehensive Methodology for Development, Parameter Estimation, and Uncertainty Analysis of Group Contribution Based Property Models-An Application to the Heat of Combustion. *J. Chem. Eng. Data* **2016**, *61* (1), 602–613.

(59) Pipke, R.; Amrhein, N. Isolation and Characterization of a Mutant of Arthrobacter Sp. Strain

GLP-1 Which Utilizes the Herbicide Glyphosate as Its Sole Source of Phosphorus and Nitrogen. *Appl. Environ. Microbiol.* **1988**, *54* (11), 2868–2870.
(60) la Cecilia, D.; Maggi, F. Analysis of Glyphosate Degradation in a Soil Microcosm. *Environ. Pollut.* **2018**, *233*, 201–207.
(61) Button, D. K. Kinetics of Nutrient-Limited Transport and Microbial Growth. *Microbiol. Rev.* **1985**, *49* (3), 270–297.
(62) la Cecilia, D.; Tang, F. H. M.; Coleman, N. V.; Conoley, C.; Vervoort, R. W.; Maggi, F. Glyphosate Dispersion, Degradation, and Aquifer Contamination in Vineyards and Wheat Fields in the Po Valley, Italy. *Water Res.* **2018**, *146*, 37–54.
(63) Muskus, A. M.; Krauss, M.; Miltner, A.; Hamer, U.; Nowak, K. M. Effect of Temperature, PH and Total Organic Carbon Variations on Microbial Turnover of 13C315N-Glyphosate in Agricultural Soil. *Sci. Total Environ.* **2019**, *658*, 697–707.
(64) Kästner, M.; Nowak, K. M.; Miltner, A.; Schäffer, A. (Multiple) Isotope Probing Approaches to Trace the Fate of Environmental Chemicals and the Formation of Non-Extractable 'Bound' Residues. *Curr. Opin. Biotechnol.* **2016**, *41*, 73–82.
(65) Fraser, F. C.; Corstanje, R.; Deeks, L. K.; Harris, J. A.; Pawlett, M.; Todman, L. C.; Whitmore, A. P.; Ritz, K. On the Origin of Carbon Dioxide Released from Rewetted Soils. *Soil Biol. Biochem.* **2016**, *101*, 1–5.
(66) Gimsing, A. L.; Borggaard, O. K.; Sestoft, P. Modeling the Kinetics of the Competitive Adsorption and Desorption of Glyphosate and Phosphate on Goethite and Gibbsite and in Soils. *Environ. Sci. Technol.* **2004**, *38* (6), 1718–1722.